

# PID-Based Sliding Mode Controller for Nonlinear Processes

Mingzhong Li, Fuli Wang, and Furong Gao\*

Department of Chemical Engineering, The Hong Kong University of Science and Technology, Clear Water Bay, Kowloon, Hong Kong

Sliding mode control (SMC) has excellent robustness to model uncertainties and disturbances. This would make SMC an ideal scheme for process control applications where model uncertainties and disturbances are common. The existing SMC, however, has the major drawback of control chattering; i.e., the controller output is a discontinuous high-frequency switching signal. This makes SMC not suitable for most chemical processes where the manipulated variables are continuous and where high-frequency changes are not permitted. To eliminate chattering, a new proportional–integral–derivative (PID)-based sliding mode control (PIDSMC) suitable for the chemical process is proposed here. The proposed control system consists of three components: a compensation of process nonlinearity, a linear feedback of state tracking errors, and a PID control of the sliding surface function. The chattering is eliminated via the replacement of the discontinuous switching in the SMC by a continuous input determined by a PID scheme. An adaptive strategy is proposed to tune the PID parameters online to control the process states onto a sliding surface that characterizes the closed-loop performance. The proposed algorithm has been shown to be effective in controlling an inverted pendulum system and a typical pH neutralization process.

## 1. Introduction

Sliding mode control (SMC),<sup>1,2</sup> a type of robust control design, has found many successful applications in servo motor control and robotics,<sup>3,4</sup> because of its performance insensitivity to model mismatches and disturbances. The design and operation of a SMC, in general, can be divided into two distinct phases: the hitting phase and the sliding phase. The controller first forces the system states onto a designed switching surface in the hitting phase; once the system states have reached the surface, the control is then switched to the sliding phase in which the states are forced to the hyperplane origin along the switching surface. In the sliding phase, the closed-loop system response is determined only by the sliding surface design, independent of model uncertainties, and system disturbances. The SMC feature of robustness to model uncertainties and the feature that the closed-loop system performance can be designed by a sliding surface should make it attractive for chemical process control as well. The existing SMC, however, has the drawback of control chattering, i.e., strong and high-frequency changes in the manipulated variable. This may not be a major problem for electrical systems. For process control, especially chemical process control, the manipulator is most likely a control valve where a high-frequency control action (chattering) is not permitted. To reduce the amplitude of control chattering, Slotine et al.<sup>5,6</sup> have proposed to replace the sliding surface with a bounded region, resulting in a SMC with boundary layers (SMCBL). However, the original SMC performance insensitivity to model uncertainties and disturbances in the sliding phase can no longer be retained in SMCBL, because the ideal sliding no longer takes place. The system states in SMCBL are driven only to the neighborhood of the sliding surface.

The other problem with the SMC design is that the bounds of uncertainties and disturbances, which are most likely not available for many practical applications, must be known in determining the SMC switching gain. Progresses such as fuzzy adaptive tuning of the switching gain by Kiriakidis et al.<sup>7</sup> and a fuzzy inference mechanism to estimate the uncertainty bound by Lin and Chiu<sup>8</sup> have been made to overcome this difficulty. These methods, however, require extensive process experience that may not be readily available in certain cases.

To overcome the chattering problem of SMC control and to eliminate the requirement of knowing the bounds of the model uncertainties and disturbances, the SMC discontinuous control input determined by the switch gain is proposed in this paper to be replaced with a continuous input determined by a proportional–integral–derivative (PID) algorithm, while the other two SMC control input terms, i.e., the process nonlinearity compensation term and the process linear state feedback term, remain unchanged. The PID proportional output drives the system to the neighborhood of the switching surface; the PID integral action forces the states to move onto the switching surface, without the requirement of the bound knowledge of uncertainties and disturbances, while the PID derivative action brings a stabilizing effect to the system by preventing excessive control action produced by the integration. It is shown in this paper that a proper selection of the integral and derivative gains can ensure the reachability condition and can eliminate the control chattering. An adaptive strategy is proposed for online tuning of the integral and derivative gains. Because the process states are forced onto the switching surface in the sliding phase, the proposed control strategy, therefore, retains the original advantages of the SMC of being insensitive to model uncertainties and disturbances. The effectiveness of the proposed system is compared with other control schemes through benchmark control problem applications—

\* To whom correspondence should be addressed. Telephone: +852-2358-7139. Fax: +852-2385-0054. E-mail: kefgao@ust.hk.

inverted pendulum and the typical chemical process of pH neutralization.

The remainder of this paper is organized as follows. Section 2 presents some background information on the existing SMC schemes and their designs. Section 3 proposes the new PID-based SMC scheme. Section 4 develops an adaptive scheme for the tuning of the PID parameters. Applications of the proposed scheme are given in section 5 to demonstrate the effectiveness in controlling uncertain nonlinear processes. Finally, conclusions are drawn in section 6.

## 2. Problem Background

We will focus on the SMC design for a class of dynamic processes that may be modeled by

$$\dot{x}^{(n)} = f(\mathbf{X}, t) + g(\mathbf{X}, t) u(t) + d(t) \quad (1)$$

where  $\mathbf{X} = [x, \dot{x}, \dots, x^{(n-1)}]^T$  is the process state vector,  $f(\mathbf{X}, t)$  and  $g(\mathbf{X}, t)$  are two unknown state functions that can be linear or nonlinear,  $u(t)$  is the control input, and  $d(t)$  is the disturbance. It should be noted that a large class of processes can be represented with this type of model structure.<sup>9</sup>

The control objective is to force the plant state vector  $\mathbf{X}$  to follow a specified desired trajectory  $\mathbf{X}_d = [x_d, \dot{x}_d, \dots, x_d^{(n-1)}]^T$ . Defining the tracking error vector  $\mathbf{X}_e = \mathbf{X} - \mathbf{X}_d$ , the problem is thus to design a control law  $u(t)$  to ensure that  $\mathbf{X}_e \rightarrow 0$  as  $t \rightarrow \infty$ . For simplicity, we assume that  $g(\mathbf{X}, t) \geq g > 0 \forall \mathbf{X}$ , where  $g$  is a constant in the subsequent development. We also assume that the functions  $f(\mathbf{X}, t)$  and  $g(\mathbf{X}, t)$  can be represented as

$$f(\mathbf{X}, t) = \hat{f}(\mathbf{X}, t) + \Delta f(\mathbf{X}, t) \quad (2)$$

$$\delta_g(\mathbf{X}, t) = \hat{g}(\mathbf{X}, t)/g(\mathbf{X}, t) \quad (3)$$

where  $\hat{f}(\mathbf{X}, t)$  and  $\Delta f(\mathbf{X}, t)$  are the estimate of  $f(\mathbf{X}, t)$  and its uncertainty,  $\hat{g}(\mathbf{X}, t)$  is the estimate of  $g(\mathbf{X}, t)$ . Many modeling techniques, such as fundamental modeling, fuzzy modeling, and neural network modeling, may be used to obtain  $\hat{f}(\mathbf{X}, t)$  and  $\hat{g}(\mathbf{X}, t)$ , and they are not the focus of this paper. Following the schemes by Slotine and Coetsee,<sup>5,6</sup> the model uncertainty and the disturbance are assumed to be bounded as below:

$$|\Delta f(\mathbf{X}, t)| \leq F \quad (4)$$

$$0 < \delta_g(\mathbf{X}, t) \leq G \quad (5)$$

and

$$|d(t)| \leq D \quad (6)$$

where  $F$ ,  $G$ , and  $D$  are constants. It should be pointed out that the general forms of  $F$  and  $G$  may be dependent on the state  $\mathbf{X}$ . The assumption of  $F$  and  $G$  being constants is to simplify the analysis notation. The adoption of the general forms of  $F$  and  $G$  will not affect the results and synthesis of the following.

A sliding surface (or a switching surface), which governs the closed-loop response in the sliding phase, is defined as follows:

$$s(\mathbf{X}_e, t) = 0 \quad (7)$$

where

$$s(\mathbf{X}_e, t) = [\Lambda^T \mathbf{1}] \mathbf{X}_e \quad (8)$$

and  $\Lambda = [\lambda_1, \lambda_2, \dots, \lambda_{n-1}]^T$  is a properly chosen coefficient vector such that  $\mathbf{X}_e$  approaches the state plane origin exponentially when  $s(\mathbf{X}_e, t)$  equals zero (i.e.,  $s^{n-1} + \lambda_{n-1}s^{n-2} + \dots + \lambda_1$  is Hurwitz). With any arbitrary initial states, the sliding mode exists if the following reachability condition is satisfied:

$$\dot{s}s \leq -\eta|s| \quad (9)$$

where  $\eta > 0$ .

As in the derivations of Kachroo et al.,<sup>10-13</sup> the SMC law takes the following form:

$$u(t) = -\frac{1}{\hat{g}(\mathbf{X}, t)}(u_f + u_L + u_V) \quad (10)$$

where

$$u_f = \hat{f}(\mathbf{X}, t) \quad (11)$$

$$u_L = [0 \ \Lambda^T] \mathbf{X}_e(t) - x_d^{(n)} \quad (12)$$

and

$$u_V = K \operatorname{sgn}[s(\mathbf{X}_e, t)] \quad (13)$$

are the process nonlinearity compensation term, the linear state feedback term, and the discontinuous sliding control term, respectively.  $\operatorname{sgn}(x)$  is a sign function. The reachability condition of eq 9 holds if the switching gain  $K$  satisfies the following:

$$K \geq |\delta_g(\Delta f + d) + (\delta_g - 1)(\hat{f} + [0 \ \Lambda^T] \mathbf{X}_e - x_d^{(n)})| + \eta \delta_g \quad (14)$$

If  $\Delta f$ ,  $\delta_g$ , and  $d$  are bounded as in eqs 4-6,  $K$  must satisfy the following to guarantee that the states reach the sliding surface:

$$K \geq G(F + D) + |G - 1| |u_f + u_L| + \eta G \quad (15)$$

The inherent drawback of this SMC design, the discontinuity in the manipulated variable, is undesirable in process control. The chattering can be reduced somewhat by introducing a bound region containing the switching surface to smooth the control behavior. In this case, the hitting phase control forces the states into the region bounded with the bounding layers, not onto the sliding surface. This idea resulted in the SMCBL.<sup>4</sup> With SMCBL, the function  $\operatorname{sgn}(s)$  in eq 13 is replaced by a saturation function,  $\operatorname{sat}(s/\Phi)$ , where  $\Phi$  is the boundary

layer thickness, and the function  $\text{sat}(x)$  is defined as

$$\text{sat}(x) = \begin{cases} x & \text{if } |x| < 1 \\ \text{sgn}(x) & \text{if } |x| \geq 1 \end{cases} \quad (16)$$

Then,  $u_v$  in eq 10 for the SMCBL becomes

$$u_v = K \text{sat}(s/\Phi) \quad (17)$$

In SMCBL, a continuous control approximating the switching signal is obtained by interpolating the control input  $u$  inside a narrow bound containing the switching surface. The SMCBL does reduce the degree of chattering in the control input; it does not altogether eliminate the chattering, as shown in section 4. At the same time, the attractive SMC feature of insensitivity to uncertainties and disturbances is lost in SMCBL because of this change. Like the original SMC, the design of SMCBL also requires prior knowledge of the bounds of uncertainties and disturbances; in practice, these bounds are rarely available. For these reasons, SMC or SMCBL is rarely used in process control.

### 3. PID-Based Sliding Mode Controller

We propose to overcome the problems associated with SMC and SMCBL in process control settings by introducing a sliding mode controller based on a PID design (PIDSMC). The original SMC structure is retained in the proposed PIDSMC, except that the discontinuous switching control input is replaced with a continuous input determined by a PID algorithm. The PID controller in the PIDSMC takes the sliding surface function  $s$  as the input, not the controlled variable as in a conventional PID control loop. The resulting overall control input of the proposed PIDSMC is

$$u(t) = -\frac{1}{g(\mathbf{X}, t)}(u_f + u_L + u_{\text{PID}}) \quad (18)$$

where  $u_f$  and  $u_L$  are the same as those defined earlier in eqs 11 and 12 and

$$u_{\text{PID}} = k_p \left( s + \frac{1}{T_i} \int s \, dt + T_d \frac{ds}{dt} \right) \quad (19)$$

where  $k_p$ ,  $T_i$ , and  $T_d$  are the PID proportional gain, integral time constant, and derivative time constant, respectively, and  $s$  is the sliding surface function. Introducing integral gain,  $k_i = k_p/T_i$ , and derivative gain,  $k_d = k_p T_d$ , results in a PID controller in terms of  $s$ :

$$u_{\text{PID}} = k_p s + k_i \int s \, dt + k_d \frac{ds}{dt} \quad (20)$$

The resulting overall structure of the proposed PID-based SMC control is schematically illustrated in Figure 1. The system consists of a nonlinear function  $u_f$  to compensate for the process nonlinearity, a linear feedback function  $u_L$  to control the process with a specified performance, and a PID controller to drive the process states onto the sliding surface. The PID proportional term drives the states to the neighborhood of the sliding surface. The PID integral action forces the states onto the sliding surface irrespective of the bounds of the uncertainties and disturbances, while the PID derivative action provides a stabilizing effect to counter the possible excessive control produced by the integral action. The integral term and the derivative term play

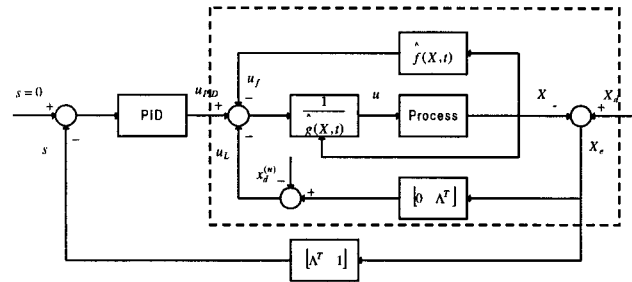


Figure 1. Proposed PIDSMC configuration.

important roles in ensuring that the states move onto the sliding surface. The working principle of the PIDSMC may be briefly explained as follows. Assume that the system is initially in the region of  $s > 0$  and that the PID proportional action term is not sufficient to drive the states toward the sliding surface. This will result in an increasing  $s$ , and the process states will move away from the surface. The integral action will increase the control action accordingly and become sufficient after a period of time to force the states to move toward the sliding surface, satisfying the reachability condition  $\dot{s}s \leq 0$ . As  $s$  approaches the sliding surface, the control action will automatically be reduced because that  $s$  is negative and  $s$  is decreasing. The reachability condition can be ensured by a proper selection of the integral and derivative gains. An online adaptive strategy is proposed in the next section to tune automatically these two parameters to ensure the reachability condition  $\dot{s}s \leq 0$ .

The proposed PIDSMC control as shown in Figure 1 consists of three major components: a nonlinear state feedback control that transforms the process into a simpler equivalent form, a linear state feedback control that completes the design of the setpoint tracking, and a PID feedback control of the sliding surface function that makes the system robust and eliminates the disturbances. In terms of the control system structure, the PIDSMC may be viewed a special case of the generalized feedback linearizing controller.<sup>14</sup> The particularities of the PIDSMC are in the use of the setpoint and the controller tuning. The outermost loop of the PIDSMC system controls the sliding behavior by setting  $s = 0$  as its setpoint. Online tuning of the PID parameters (as described in section 4) ensures quick hitting of the system states onto the sliding surface. The first two components, enclosed by the dashed line in Figure 1, in essence may also be viewed as a combination of a nonlinear state feedback and a linear feedback control. The components inside the dashed line box alone may be used for certain process control applications. However, that would require the process model to be reasonably accurate; any model inaccuracy would present possible stability problems. Furthermore, the two components alone in the dashed line box would have poor disturbance rejection as well. The addition of the PID control of the sliding surface function allows the overall system to be more robust and to have a more consistent performance as the system states are forced onto the sliding surface. Because the PID output is continuous, the SMC control chattering is eliminated.

### 4. Online Tuning of the Integral and Derivative Gains

Assume that, for a given proportional gain, there exist an integral gain  $K_i^*$  and a derivative gain  $K_d^*$  such that

the reachability condition is satisfied, i.e., with  $u_{PID} = k_p s + k_i^* \int s dt + k_d^* (ds/dt)$ , the condition  $\dot{s}s < -\eta|s|$  holds.

Define the PID parameter errors as

$$\tilde{K}_i = K_i - K_i^* \quad (21)$$

$$\tilde{K}_d = K_d - K_d^* \quad (22)$$

Choose a Lyapunov function as

$$V = \frac{1}{2} \left( s^2 + \frac{1}{\alpha_1} \tilde{K}_i^2 + \frac{1}{\alpha_2} \tilde{K}_d^2 \right) \quad (23)$$

where  $\alpha_1$  and  $\alpha_2$  are positive constants. Differentiation of  $V$  with respect to time results in the following equation:

$$\dot{V} = s\dot{s} + \frac{1}{\alpha_1} \tilde{K}_i \dot{\tilde{K}}_i + \frac{1}{\alpha_2} \tilde{K}_d \dot{\tilde{K}}_d \quad (24)$$

Substituting eqs 1, 8, and 20 into eq 24 results in

$$\begin{aligned} \dot{V} = & \frac{1}{\delta_g} s \{ \delta_g [\Delta f + d(t)] + (\delta_g - 1)(\dot{f} + u_L) - u_{PID} \} + \\ & \frac{1}{\alpha_1} \tilde{K}_i \dot{\tilde{K}}_i + \frac{1}{\alpha_2} \tilde{K}_d \dot{\tilde{K}}_d = \frac{1}{\delta_g} s \{ \delta_g [\Delta f + d(t)] + \\ & (\delta_g - 1)(\dot{f} + u_L) - (K_p s + K_i^* \int s + K_d^* \dot{s}) \} - \\ & \frac{1}{\delta_g} s (K_i \int s + K_d \dot{s} - K_i^* \int s - K_d^* \dot{s}) + \frac{1}{\alpha_1} \tilde{K}_i \dot{\tilde{K}}_i + \frac{1}{\alpha_2} \tilde{K}_d \dot{\tilde{K}}_d = \\ & - \frac{\eta}{\delta_g} |s| - \frac{1}{\delta_g} \tilde{K}_i s \int s - \frac{1}{\delta_g} \tilde{K}_d s \dot{s} + \frac{1}{\alpha_1} \tilde{K}_i \dot{\tilde{K}}_i + \frac{1}{\alpha_2} \tilde{K}_d \dot{\tilde{K}}_d = \\ & - \frac{\eta}{\delta_g} |s| - \tilde{K}_i \left( \frac{1}{\delta_g} s \int s - \frac{1}{\alpha_1} \dot{\tilde{K}}_i \right) - \tilde{K}_d \left( \frac{1}{\delta_g} s \dot{s} - \frac{1}{\alpha_2} \dot{\tilde{K}}_d \right) \quad (25) \end{aligned}$$

Hence, the adaptive laws for  $K_i$  and  $K_d$  can be obtained as follows:

$$\dot{\tilde{K}}_i = \frac{\alpha_1}{\delta_g} s \int s = \gamma_1 s \int s \quad (26)$$

$$\dot{\tilde{K}}_d = \frac{\alpha_2}{\delta_g} s \dot{s} = \gamma_2 s \dot{s} \quad (27)$$

where  $\gamma_1 = \alpha_1/\delta_g$  and  $\gamma_2 = \alpha_2/\delta_g$ .

From eqs 26 and 27, the PID's integral and derivative gains can be automatically tuned to satisfy the reachability condition. Hence, the stability of the closed-loop system can be guaranteed as long as the integral and derivative gains are tuned according to eqs 26 and 27. This conclusion is based on the assumption of the existence of a set of PID parameters that satisfy the reachability condition. The condition of the existence of such a set of PID parameters is an important issue; it will be the topic of subsequent research in this area. At this point, simulations show that this assumption is true for a large class of nonlinear processes.

## 5. Simulation Results

The proposed PIDSMC is applied first to control an inverted pendulum, followed by a comparison control

application with a nonlinear internal model control (IMC) controller.<sup>24</sup> The simulations are conducted in the MATLAB (version 5.2) with a Simulink environment. In all cases,  $\gamma_1$  and  $\gamma_2$  are selected to be 0.01 for simplicity.

**Case 1: Inverted Pendulum.** The results of controlling an inverted pendulum with the proposed algorithm are compared with those of a PID control, the original SMC, and SMCBL.

The inverted pendulum system, a common benchmark control problem, has a nonlinear time-varying dynamic such as the following:

$$\ddot{x} + b\dot{x} + a \cos(x) = u + d(t) \quad (28)$$

The true process parameters are  $a = 3.2$ ,  $b = 0.5 + 0.2 \sin(t)$ , and the disturbance  $d(t) = 2 \sin(0.1t)$ . Because of modeling error, we assume that the estimated model is  $\hat{f}(x,t) = -0.5x - 3.5 \cos(x)$ . It is obvious that the estimated model is significantly different from the true process of  $f(x,t) = -[0.5 + 0.2 \sin(t)]x - 3.2 \cos(x)$ . Four different types of controllers, PID, SMC, SMCBL, and the proposed PIDSMC, are designed and tested to track the setpoint trajectory,  $x_d(t) = \sin(0.2t)$ . The parameters of the PID control are fine-tuned as  $K_a = 4$ ,  $K_i = 0.2$ , and  $K_d = 0.5$ . The SMC parameters are set as  $\lambda = 2$  and  $K_V = 3.5$ . The SMCBL parameters are set as  $\lambda = 2$ ,  $K_V = 3.5$ , and  $\Phi = 0.01$ . The PIDSMC parameters are set as  $K_p = 4$  and  $\lambda = 2$ , and the initial integral and derivative gains are  $K_i = 0.2$  and  $K_d = 0.6$ , respectively. The control responses of these four controllers are shown in Figure 2. It can be seen that the PID controller failed to control the nonlinear process, because the process output is oscillatory. The process is controlled reasonably well by the SMC in tracking the setpoint trajectory. The manipulated variable, however, has very strong high-frequency changes, exhibiting serious control chattering as expected. The control chattering is reduced somewhat with the SMCBL in comparison with the SMC, but this is at the cost of the deterioration of the tracking performance as shown in Figure 2e. The PIDSMC effectively controls the process to follow closely the setpoint profile without any control chattering. The superiority of the PIDSMC in setpoint tracking is clearly illustrated with this simulation. To test the robustness of the PIDSMC, the estimated process model and disturbance are changed to  $\hat{f}(x,t) = 0.4x - 3 \cos(x)$  and  $d(t) = 3 \sin(0.1t)$ , respectively, while all of the controller design parameters remain unchanged. With this poor model, the inequality (15) does not hold for the SMC. The control responses with the SMC and SMCBL become divergent, so they are not plotted. On the other hand, the proposed PIDSMC still works very well, as is illustrated in Figure 3, suggesting the proposed PIDSMC's superior robustness to uncertainties in the model and disturbances.

**Case 2: Control of a pH Neutralization Process.** Control of pH neutralization is a well-known problem, because of the strong process nonlinearity around the neutrality point at pH = 7. A number of control strategies have been proposed. They may be broadly classified into linear model based controls and nonlinear model based controls. The linear model based controls tackle the process nonlinearity by viewing the process as a linear time-varying system; this leads naturally to linear adaptive controls.<sup>16-18</sup> The nonlinear controls are designed based on nonlinear models,<sup>19-24</sup> resulting often in more effective nonlinearity compensation and better

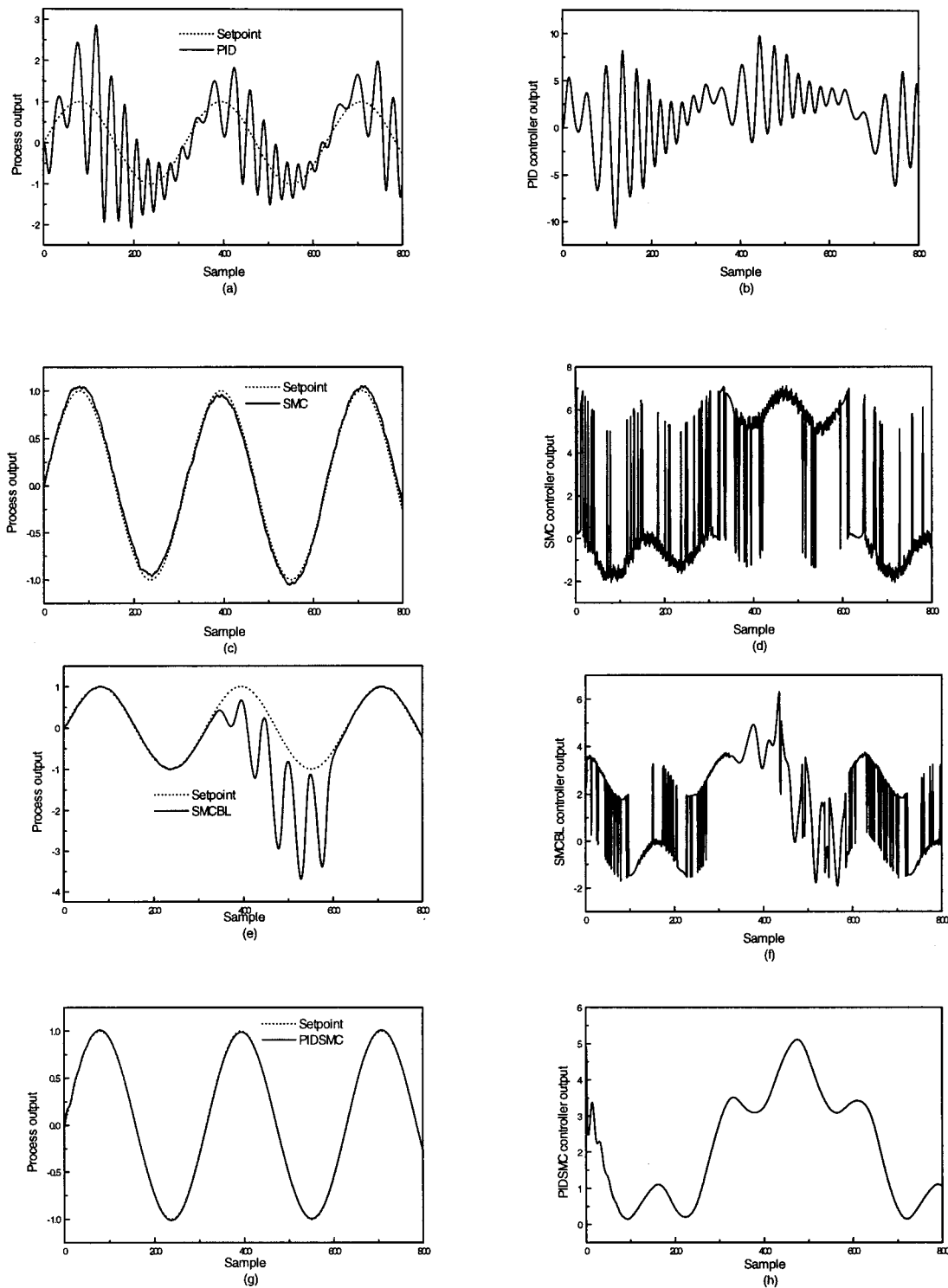


**Figure 2.** Control response comparison for an inverted pendulum.

robustness. Among these nonlinear pH controls, the following are based on fundamental principles. Gustafsson and Waller<sup>22</sup> proposed a state model based on the fundamental balances for a pH process, resulting in a nonlinear model based feedback and feedforward pH control. Wright and Kravaris<sup>23</sup> defined the strong acid equivalent for the pH process, resulting in a control based on a minimal order realization of the model. Kulkarni and Tambe<sup>24</sup> proposed a nonlinear IMC control for pH control. The success of these above strategies depends largely on the accuracy of the model developed. It can be expected that the control performance will

deteriorate with the presence of the model errors. In the following, we compare the effectiveness of the proposed PIDSMC control with a nonlinear IMC control<sup>24</sup> as a representative of those nonlinear model based controls.

**(1) pH Neutralization Process.** The neutralization process can take place in a continuously stirred tank reactor as shown in Figure 4. Hydrogen chloride (HCl) is fed into the mixing tank with volumetric flow rate  $F_1$  and concentration  $C_{Cl_1}$ . Sodium hydroxide (NaOH) is fed at flow rate  $F_2$  and concentration  $C_{Na_2}$  to control the pH of the effluent stream. The first principles model of the

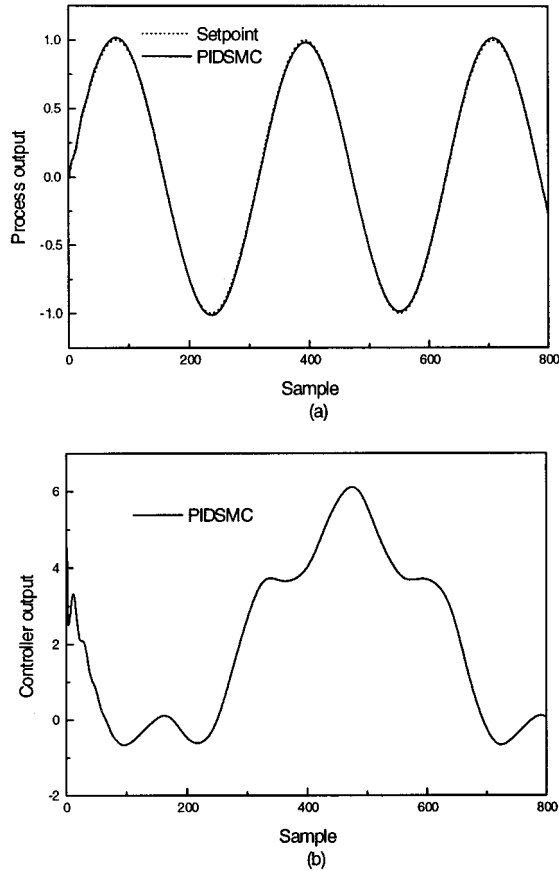


**Figure 3.** Robustness demonstration of the proposed PIDSMC system is derived as<sup>15</sup>

$$F(t) = F_1(t) + F_2(t) \quad (29)$$

$$\frac{dC_{Cl}(t)}{dt} = \frac{1}{V}[F_1(t) C_{Cl_1}(t) - F(t) C_{Cl}(t)] \quad (30)$$

$$\frac{dC_{Na}(t)}{dt} = \frac{1}{V}[F_2(t) C_{Na_2}(t) - F(t) C_{Na}(t)] \quad (31)$$

$$K_w = C_H C_{OH} \quad (32)$$

$$C_{OH}(t) = C_H(t) + C_{Na}(t) - C_{Cl}(t) \quad (33)$$

$$\text{pH} = -\log C_H \quad (34)$$

$F_2$  is manipulated to maintain the effluent pH at a desired value.

From eqs 29–33, we have

$$\frac{dC_H(t)}{dt} = \frac{K_w C_H + C_{Cl_1} C_H^2 - C_H^3}{V(K_w + C_H^2)} F_1 + \frac{K_w C_H - C_{Na_2} C_H^2 - C_H^3}{V(K_w + C_H^2)} F_2 \quad (35)$$

Let

$$\bar{C}_H = \frac{C_H}{C_H^s}, \quad \bar{C}_{Na_2} = \frac{C_{Na_2}}{C_H^s}, \quad \bar{C}_{Cl_1} = \frac{C_{Cl_1}}{C_H^s} \quad (36)$$

where  $C_H^s = 10^{-7}$ . The above can be represented in

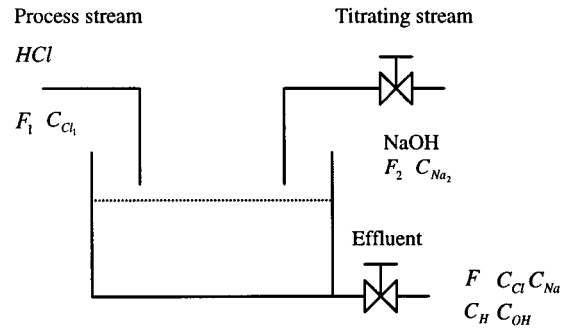


**Figure 4.** pH neutralization process.<sup>24</sup>

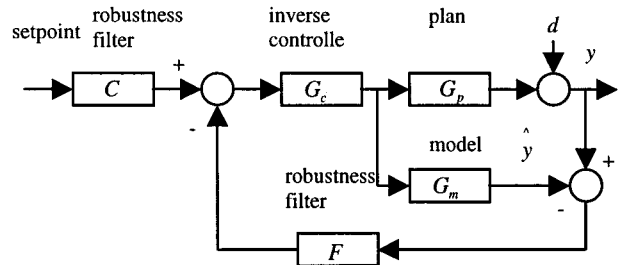


**Figure 5.** Nonlinear IMC.

**Table 1. Parameters Used in the pH Neutralization Control Simulation<sup>24</sup>**

variable	meaning	setting
$V$	volume of the tank	$2.0 \times 10^4$ L
$F_1$	flow rate of the acid	$5.0 \times 10^2$ L/min
$F_2$	flow rate of the base	$5.0 \times 10^1$ L/min
$C_{Cl_1}$	concn of the acid in $F_1$	0.01 gmol/L
$C_{Na_2}$	concn of the base in $F_2$	0.1 gmol/L
$K_w$	water equilibrium constant	$10^{-14}$ (gmol/L) <sup>2</sup>
$C_H$	hydrogen concn	gmol/L

dimensionless form as below:

$$\frac{d\bar{C}_H(t)}{dt} = \frac{\bar{C}_H + \bar{C}_{Cl_1} \bar{C}_H^2 - \bar{C}_H^3}{V(1 + \bar{C}_H^2)} F_1 + \frac{\bar{C}_H + \bar{C}_{Na_2} \bar{C}_H^2 - \bar{C}_H^3}{V(1 + \bar{C}_H^2)} F_2 \quad (37)$$

From eqs 34 and 37, we have

$$\text{pH} = - \frac{10^{7-\text{pH}} + \bar{C}_{Cl_1} \times 10^{14-2\text{pH}} - 10^{21-3\text{pH}}}{V \ln 10(1 + 10^{14-2\text{pH}})} F_1 - \frac{10^{7-\text{pH}} + \bar{C}_{Na_2} \times 10^{14-2\text{pH}} - 10^{21-3\text{pH}}}{V \ln 10(1 + 10^{14-2\text{pH}})} F_2 \quad (38)$$

**(2) Comparison Results.** A nonlinear IMC, a model-based control, of the structure as shown in Figure 5 is adopted for comparison with the proposed PIDSMC.  $G_c$  is commonly chosen as the inverse of the internal model  $G_m$ .

In the simulation, the nominal settings of Kulkarni and Tambe<sup>24</sup> for the pH neutralization process are adopted, as shown in Table 1. The operating range of the base inlet stream  $F_2$  is 0–100 L/min. The initial pH value is 7. For the first simulation, a perfect model is assumed, i.e.,  $\hat{f} = F_1[(10^{7-\text{pH}} + \bar{C}_{Cl_1} \times 10^{14-2\text{pH}} - 10^{21-3\text{pH}})]/[V \ln 10(1 + 10^{14-2\text{pH}})]$  and  $\hat{g} = -[(10^{7-\text{pH}} + \bar{C}_{Na_2} \times 10^{14-2\text{pH}} - 10^{21-3\text{pH}})]/[V \ln 10(1 + 10^{14-2\text{pH}})]$ . The

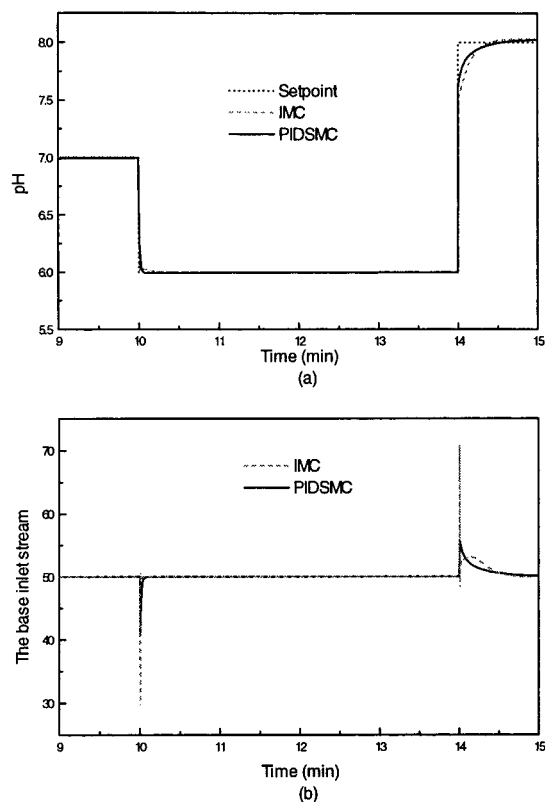


**Figure 6.** pH neutralization control based on the perfect model.

IMC control is designed with filters  $F = 1$  and  $C(t) = 1 - e^{-At}$ , where  $A$  is adjusted to be 1.43 for a fast setpoint tracking performance. The PIDSMC is designed with  $K_p = 2$ ,  $\lambda = 2$ , and the initial integral and derivative gains of  $K_i = 0.15$  and  $K_d = 0.04$ , respectively. The performances of the PIDSMC and IMC controls are compared to track the setpoint profile as shown in Figure 6. A negative step change in the setpoint is introduced at  $t = 10$ , changing the pH from the neutralization point of  $\text{pH} = 7$  to that of  $\text{pH} = 6$ , followed by a positive step at  $t = 14$ , changing the pH from 6 to 8. Both controls perform well in this case, as the responses can track the setpoint closely as evidenced in Figure 6a. Examination of the manipulated variable responses (Figure 6b) indicates that the PIDSMC produces less dramatic changes in the manipulated variable for the same setpoint step changes. With the settings for both controllers unchanged, the second simulation compares the disturbance rejection ability of these two schemes. A disturbance is introduced by changing the concentration  $C_{\text{Na}_2}$  from the nominal 0.01 to 0.015 gmol/L at  $t = 10$ . The control responses of the PIDSMC and IMC are shown in Figure 7. With this strong disturbance, the PIDSMC can drive the process pH value back to the setpoint without overshoot within a short period of time (about 20 s). The nonlinear IMC takes a long time (about 180 s) to recover to the set pH value. This clearly shows that PIDSMC has a better ability to reject a disturbance. The third simulation tests the control performance with an imperfect model, so that the robustness of these two controllers can be compared. The settings of both controllers are unchanged. Now, an imperfect model with  $\hat{f} = F_1[(10^{7-\text{pH}} + 0.8\bar{C}_{\text{Cl}_1} \times 10^{14-2\text{pH}} - 10^{21-3\text{pH}})/[V \ln 10(1 + 10^{14-2\text{pH}})]]$  and  $\hat{g} = -[(10^{7-\text{pH}} - 0.9\bar{C}_{\text{Na}_2} \times 10^{14-2\text{pH}} - 10^{21-3\text{pH}})/[V \ln 10(1 + 10^{14-2\text{pH}})]]$  is used for the process simulation, with the results shown in Figure 8. With this imperfect

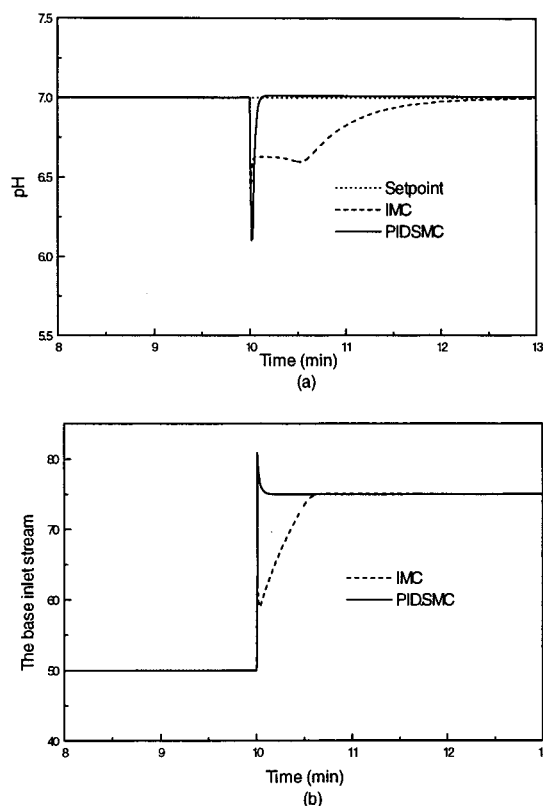


**Figure 7.** Disturbance rejection control comparison.

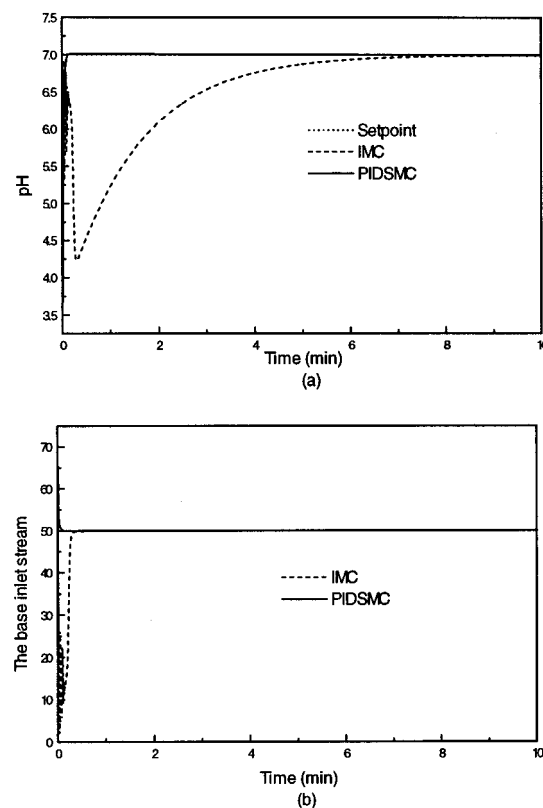


**Figure 8.** pH neutralization control based on an imperfect model.

model, the nonlinear IMC takes an excessive long time to respond to a setpoint change and it has strong oscillations in the controlled variable. The PIDSMC can still track the setpoint very well without any oscillation. This excellent robustness may be due to the inherent robust nature of the PIDSMC and its tuning algorithm.

The online tuning of PID parameters provides a quick and smooth hitting of the system states onto the sliding surface.

The above simulations suggest that a typical strong nonlinear process such as the pH neutralization process can be effectively controlled without any chattering by the proposed PIDSMC with fast setpoint tracking and good disturbance rejection.

## 6. Conclusions

A PID-based SMC (PIDSMC) has been proposed for nonlinear process applications. Simulations show that the proposed PIDSMC has excellent robustness to model uncertainty and it does not have the drawback of the control chattering associated with SMC.

## Nomenclature

$\mathbf{X} = [x, \dot{x}, \dots, x^{(n-1)}]^T$  = process state vector  
 $f(\mathbf{X}, t)$  = unknown state function  
 $\hat{f}(\mathbf{X}, t)$  = estimate of  $f(\mathbf{X}, t)$   
 $\Delta f(\mathbf{X}, t)$  = uncertainty of  $f(\mathbf{X}, t)$   
 $F$  = bound of  $f(\mathbf{X}, t)$   
 $g(\mathbf{X}, t)$  = unknown state function  
 $\hat{g}(\mathbf{X}, t)$  = estimate of  $g(\mathbf{X}, t)$   
 $\delta_g(\mathbf{X}, t) = \hat{g}(\mathbf{X}, t)/g(\mathbf{X}, t)$  = function as defined  
 $G$  = bound of  $\delta_g(\mathbf{X}, t)$   
 $d(t)$  = disturbance  
 $D$  = bound of  $d(t)$   
 $u(t)$  = control input  
 $d(t)$  = disturbance  
 $\mathbf{X}_d = [x_d, \dot{x}_d, \dots, x_d^{(n-1)}]^T$  = desired trajectory  
 $\mathbf{X}_e = \mathbf{X} - \mathbf{X}_d$  = tracking error vector  
 $s(\mathbf{X}_e, t) = [\Lambda^T \ 1]\mathbf{X}_e$  = sliding surface  
 $\Lambda = [\lambda_1, \lambda_2, \dots, \lambda_{n-1}]^T$  = coefficient vector  
 $\eta$  = positive constant in reachability condition  
 $u_f = f(\mathbf{X}, t)$  = process nonlinearity in the compensation term  
 $u_L = [0 \ \Lambda^T]\mathbf{X}_e(t) - x_d^{(m)}$  = linear state feedback term  
 $u_V = K \operatorname{sgn}(s(\mathbf{X}_e, t))$  = discontinuous sliding control term  
 $K$  = gain of the switching control  
 $\operatorname{sgn}(x)$  = sign function  
 $\operatorname{sat}(x)$  = saturation function  
 $k_p$  = proportional gain  
 $T_i$  = integral time constant  
 $T_d$  = derivative time constant  
 $k_i = k_p/T_i$  = integral gain  
 $k_d = k_p T_d$  = derivative gain  
 $\dot{\hat{K}}_i = (\alpha_1/\delta_g) s f s = \gamma_1 s f s$  = adaptive law for  $K_i$   
 $\dot{\hat{K}}_d = (\alpha_2/\delta_g) s \dot{s} = \gamma_2 s \dot{s}$  = adaptive law for  $K_d$   
 $V = 1/2(s^2 + (1/\alpha_1)\hat{K}_i^2 + (1/\alpha_2)\hat{K}_d^2)$  = Lyapunov function  
 $\alpha_1, \alpha_2$  = positive constants  
 $\gamma_1$  = learning rate for the integral gain  
 $\gamma_2$  = learning rate for the derivative gain

## Literature Cited

- (1) Utkon, V. I. Variable structure systems with sliding modes. *IEEE Trans. Autom. Control* **1977**, *22*, 212–222.
- (2) Edwards, C.; Spurgeon, S. K. *Sliding mode control: theory and applications*; Taylor & Francis Ltd.: London, 1998.

- (3) Hashimoto, H.; Yamamoto, H.; Yanagisawa, S.; Harashima, F. Brushless servomotor control using variable structure approach. *IEEE Trans. Ind. Appl.* **1988**, *24* (1), 160–170.
- (4) Slotine, J. J. E.; Sastry, S. S. Tracking control of nonlinear systems using sliding surfaces with application to robot manipulators. *Int. J. Control* **1983**, *38* (2), 465–492.
- (5) Slotine, J.-J. E. Sliding controller design for nonlinear systems. *Int. J. Control* **1984**, *40* (2), 421–434.
- (6) Slotine, J. J. E.; Coetsee, J. A. Adaptive sliding controller synthesis for nonlinear systems. *Int. J. Control* **1986**, *43* (6), 1631–1651.
- (7) Kiriakidis, K.; Tzes, A.; Grivas, A.; Peng, P. Y. Modeling, plant uncertainties, and fuzzy logic sliding control of gaseous systems. *IEEE Trans. Control Syst. Technol.* **1999**, *7* (1), 42–55.
- (8) Lin, F. J.; Chiu, S. L. Adaptive fuzzy sliding-mode control for PM synchronous servo motor drives. *IEE Proc. Control Theory* **1998**, *145* (1), 63–72.
- (9) Isidori, A. *Nonlinear control systems: an introduction*, 2nd ed.; Springer-Verlag: Berlin, 1989.
- (10) Kachroo, P. Existence of solutions to a class of nonlinear convergent chattering-free sliding mode control systems. *IEEE Trans. Autom. Control* **1999**, *44* (8), 1620–1624.
- (11) Chan, C. Y. Discrete adaptive sliding mode control of a class of stochastic systems. *Automatica* **1999**, *35* (8), 1491–1498.
- (12) Colantonio, M. C.; Desases, A. C.; Romagnoli, J. A.; Palazoglu, A. Nonlinear control of a CSTR: disturbance rejection using sliding mode control. *Ind. Eng. Chem. Res.* **1995**, *34*, 2383–2392.
- (13) Sira-Ramirez, H. Sliding regimes in general nonlinear systems: a relative degree approach. *Int. J. Control* **1989**, *50*, 1487–1506.
- (14) Kravaris, C.; Chung, C. B. Nonlinear state feedback synthesis by global input/output Linearization. *AIChE J.* **1987**, *33*, 592–603.
- (15) Smith, C. A.; Corripio, A. B. *Principles and practice of automatic process control*; John Wiley & Sons: New York, 1985.
- (16) Mellichamp, D. A.; Coughanowr, D. R.; Koppel, L. B. Characterization and gain identification of time varying flow processes. *AIChE J.* **1966**, *12*, 75–82.
- (17) Gupta, S. R.; Coughanowr, D. R. On-line gain identification of flow processes with application to adaptive pH control. *AIChE J.* **1978**, *24*, 654–664.
- (18) Buchholt, F.; Kummel, M. Self-tuning control of a pH-neutralization process. *Automatica* **1979**, *15*, 665–671.
- (19) Fruzzetti, K. P.; Palazoglu, A.; McDonald, K. A. Nonlinear model predictive control using Hammerstein models. *J. Process Control* **1997**, *7*, 31–41.
- (20) Proll, T.; Karim, M. N. Model-predictive pH control using real-time NARX approach. *AIChE J.* **1994**, *40*, 269–282.
- (21) Norquay, S. J.; Palazoglu, A.; Romagnoli, J. A. Application of Wiener model predictive control (WMPC) to a pH neutralization experiment. *IEEE Trans. Control Syst. Technol.* **1999**, *7* (4), 437–445.
- (22) Gustafsson, T. K.; Waller, K. V. Dynamic modeling and reaction invariant control of pH. *Chem. Eng. Sci.* **1983**, *38*, 389–398.
- (23) Wright, R. A.; Kravaris, C. Nonlinear control of pH process using the strong acid equivalent. *Ind. Eng. Chem. Res.* **1991**, *30*, 1561–1572.
- (24) Kulkarni, B. D.; Tambe, S. S. Nonlinear pH control. *Chem. Eng. Sci.* **1991**, *46* (4), 995–1003.

Received for review September 27, 1999

Revised manuscript received December 15, 2000

Accepted March 30, 2001

IE990715E